Waste Management 161 (2023) 29–42

Contents lists available at ScienceDirect

Waste Management

journal homepage: www.elsevier.com/locate/wasman

Inhibitory mechanisms on dry anaerobic digestion: Ammonia, hydrogen and propionic acid relationship

Ildefonso Rocamora [a], Stuart T. Wagland [a], Francis Hassard [a], Raffaella Villa [a,b], Miriam Peces [c], Edmon W. Simpson [d], Oliver Fernández [d], Yadira Bajón-Fernández [a,e,*]

[a] School of Water, Energy and Environment, Cranfield University, Bedford, UK
[b] De Montfort University, School of Engineering and Sustainable Development, UK
[c] Department of Chemical Engineering and Analytical Chemistry, University of Barcelona, 08028 Barcelona, Spain
[d] Amey PLC., Oxford, UK
[e] Institute for Nanotechnology and Water Sustainability, College of Science, Engineering and Technology, University of South Africa, Johannesburg 1710, Florida, South Africa

ARTICLE INFO

Keywords:
Propionic accumulation
Syntrophic acetogenic oxidation
Butyric accumulation
Methanoculleus
High solids digestion
Hydrogen inhibition

ABSTRACT

Inhibitory pathways in dry anaerobic digestion are still understudied and current knowledge on wet processes cannot be easily transferred. This study forced instability in pilot-scale digesters by operating at short retention times (40 and 33 days) in order to understand inhibition pathways over long term operation (145 days). The first sign of inhibition at elevated total ammonia concentrations (8 g/l) was a headspace hydrogen level over the thermodynamic limit for propionic degradation, causing propionic accumulation. The combined inhibitory effect of propionic and ammonia accumulation resulted in further increased hydrogen partial pressures and *n*-butyric accumulation. The relative abundance of *Methanosarcina* increased while that of *Methanoculleus* decreased as digestion deteriorated. It was hypothesized that high ammonia, total solids and organic loading rate inhibited syntrophic acetate oxidisers, increasing their doubling time and resulting in its wash out, which in turn inhibited hydrogenotrophic methanogenesis and shifted the predominant methanogenic pathway towards acetoclastic methanogenesis at free ammonia over 1.5 g/l. C/N increases to 25 and 29 reduced inhibitors accumulation but did not avoid inhibition or the washout of syntrophic acetate oxidising bacteria.

1. Introduction

Food waste (FW) production in the EU alone reaches around 88 million tonnes annually, which accounts for ca. 20 % of all the food produced in the EU (EU, 2021). Waste production and its landfilling remain high despite the efforts of governments and society to reduce them in recent years (EC, 2020), posing opportunities to seek treatment alternatives with an environmental and economic benefit. Dry anaerobic digestion (AD) is a popular solution for this problem, as it is known to be a successful process to treat organic wastes like green waste, agricultural waste, FW or the organic fraction of municipal solid waste (OFMSW) (Rocamora et al., 2020), also reducing pressure on biofuels production from food (Shams Esfandabadi et al., 2022). This is reflected by the increasing number of plants registered in the last few years in countries like the United Kingdom (ADBA, 2021).

Dry AD takes place at total solids (TS) ranging between 20 % and 50 % inside the reactors (Karthikeyan and Visvanathan, 2013; Rocamora et al., 2020). This translates in the use of low amounts of water when treating organic solid wastes like OFMSW, with an associated economic and environmental benefit when compared to wet AD. Higher TS content translates into higher methane productions per volume of digester and more compact treatment plants than those using wet AD. Nonetheless, high TS content is also linked to some operational problems. The main disadvantages are diverse, including the longer degradation time

Abbreviations: α_c, Apparent fractionation factor; AD, Anaerobic digestion; C/N, Carbon to nitrogen ratio; DBLM, Distance-based linear modelling; FA, Free ammonia; FW, Food waste; OFMSW, Organic fraction of municipal solid waste; OLR, Organic loading rate; PCoA, Principal coordinate ordination analysis; RR, Ripley ratio; RT, Retention time; SAB, Syntrophic acetogenic bacteria; SAOB, Syntrophic acetate oxidising bacteria; SOPB, Syntrophic propionate oxidizing bacteria; TE, Trace element; TAN, Total ammonia nitrogen; TS, Total solids; VFA, Volatile fatty acids.

* Corresponding author at: School of Water, Energy and Environment, Cranfield University, Bedford, UK.
E-mail address: y.bajonfernandez@cranfield.ac.uk (Y. Bajón-Fernández).

https://doi.org/10.1016/j.wasman.2023.02.009
Received 11 August 2022; Received in revised form 10 January 2023; Accepted 9 February 2023
Available online 28 February 2023

of the organic matter resulting in increased lag phases; or the accumulation of volatile fatty acids (VFA) and free ammonia (FA) due to the higher TS, reduced moisture and lack of mixing compared to wet AD (Rocamora et al., 2020).

Inhibitory problems are a common concern when feedstocks like OFMSW or FW are digested, as their low carbon to nitrogen ratio (C/N) can result in nitrogen build-up in the form of total ammonia nitrogen (TAN) (Yirong et al., 2017). TAN refers to the sum of FA and ammonium, with temperature and pH determining the relative presence as ammonium or FA in the equilibrium (Capson-Tojo et al., 2020). FA is considered as the more toxic form, as it will easily diffuse through the cell wall of microorganisms and convert to ammonium due to the low intracellular pH, causing imbalances (Kayhanian, 1999). To maintain intracellular pH, the cells will activate the potassium pump to reduce the number of cations, increasing the cell energy requirements (Yan et al., 2020). If the cell cannot sustain a constant pH due to ammonium accumulation, this process will lead to cytotoxicity (Jiang et al., 2019; Sprott et al., 1984; Sprott and Patel, 1986), preventing cell activity and resulting in digester failure.

Ammonia inhibitory levels remain unclear, with some authors reporting values as TAN instead of FA, and different concentrations having different impacts depending on the methanogenic communities (Jiang et al., 2019). Authors seem to agree in reporting strict hydrogenotrophic and versatile archaea utilising the hydrogenotrophic pathway, like *Methanosarcina*, as more resistant than strict acetoclastic archaea (Angelidaki and Ahring, 1993; Fotidis et al., 2014a). This higher tolerance is responsible for the shift of methane production towards the hydrogenotrophic pathway at high FA contents, which is usually the case for FW or OFMSW digestion (Yirong et al., 2017). In this pathway VFA are converted through beta-oxidation to acetate and hydrogen by syntrophic acetogenic bacteria (SAB), while acetate is converted by syntrophic acetate oxidising bacteria (SAOB) to H_2 and CO_2 (Eq. 1). These products are then converted by hydrogenotrophic archaea to methane (Westerholm et al., 2019) (Eq. 2). VFA oxidation are thermodynamically unfavoured reactions; only possible by the syntrophic relation of bacteria and hydrogenotrophic archaea. To make the reaction energetically favourable, the products of each reaction need to be consumed by the next step in the chain, keeping intermediates at low concentrations (Müller et al., 2010; Schink, 1997).

$$CH_3COO^- + H^+ + 2H_2O \leftrightarrows 2CO_2 + 4H_2 \quad (1)$$

$$4H_2 + CO_2 \rightarrow CH_4 + 2H_2O \quad (2)$$

High FA contents increase energy requirements to maintain intracellular pH (Yan et al., 2020), hindering methane production and growth rate of methanogens and SAOB (Fotidis et al., 2013), which have a slower duplication time and require longer retention times (RT) (Schnürer and Nordberg, 2008). Hence, ADs generating methane predominantly by hydrogenotrophic pathway are more exposed to inhibitory problems and have a reduced resilience compared to ADs with contribution from both acetoclastic and hydrogenotrophic methanogens (Jiang et al., 2019).

One of the most commonly reported signs of ammonia inhibition is the accumulation of VFAs (Banks et al., 2012), which can lead to inhibition of methanogens (Ahring and Westermann, 1988) and even the acidification of the system (Siegert and Banks, 2005). Accumulation of propionic acid is the first sign of inhibition, although the reasons for its build up are not completely clear and different hypotheses have been proposed in literature. Propionic acid is generated during the acidogenesis phase and converted to acetate by syntrophic propionate oxidizing bacteria (SPOB) (Eq. 3) prior its consumption in the hydrogenotrophic pathway (Eq. 1).

$$CH_3CH_2COO^- + 2H_2O \leftrightarrows CH_3COO^- + CO_2 + 3H_2 \quad (3)$$

Propionic oxidation into acetate is the most thermodynamically unfavoured reaction of this chain, and hence the first to show inhibitory problems (Stams and Plugge, 2009). Different hypotheses for propionic accumulation have been postulated for wet AD, with some literature identifying hydrogen partial pressure over 10^{-4} bar as responsible for the thermodynamic blockage of propionic degradation (Gujer and Zehnder, 1983). However, deficiency of trace elements (TE) like Fe, Ni, Se, W or Co is reported as another cause for this accumulation (Banks et al., 2012; Choong et al., 2016). TE are essential for enzymes and cofactors required in the relation between syntrophic bacteria and methanogens, making possible propionic degradation and the hydrogenotrophic pathway (Westerholm et al., 2015). Therefore, it was hypothesized that hydrogen partial pressure increase would just be a by-product of propionic degradation, and not its cause (Banks et al., 2012). Further research is necessary to clarify these hypotheses in dry AD, where the effect of the high TS on the inhibitory mechanisms leading to digester instability and eventual failure of the ADs remain still unclear.

One of the recurrent solutions in literature to reduce ammonia accumulation when digesting feedstocks like FW or OFMSW is to increase the C/N ratio by co-digestion with materials with high carbon content, like paper (Kim and Oh, 2011), cardboard (Capson-tojo et al., 2017) or green waste (Kumar et al., 2010). Zeshan et al. (2012) reduced TAN by 30 % and increased methane production over 50 % by increasing the C/N from 27 to 32 when digesting simulated OFMSW with green waste and paper waste at TS of 20 %. Zhang et al. (2012) reduced TAN from 3.5 g/l to under 1 g/l achieving stable operation by increasing the C/N ratio form 11 to 29 while co-digesting FW and cardboard packaging in wet digestion (TS < 7 %) at mesophilic conditions. However, literature is scarce at TS contents over 40 %, where mixing is limited and homogeneity is lower compared to other dry AD processes where internal mixing is still possible.

This study investigated the inhibition mechanisms in dry AD (>40 %) at high TAN and FA contents, providing knowledge for future research to develop operational strategies that can reduce ammonia inhibition and propionic accumulation. Two different experiments were performed: i) digestion of OFMSW with reducing RT and therefore increasing organic loading rates (OLR) that force instability and unravel inhibition and failure mechanisms and ii) co-digestion of OFMSW with paper to elucidate the impact of increasing C/N ratio on inhibition pathways.

2. Materials and methods

2.1. Feedstock and inoculum

The solid inoculum (digestate) and the substrate (OFMSW) used in the different experiments were obtained from a semi-continuous dry AD facility operating at mesophilic conditions in North-East England, United Kingdom, treating up to 40,000 tonnes of OFMSW per year. The OFMSW was mechanically recovered on site from house residue and reduced with a shredder to a particle size < 40 mm. Inoculum and feedstock were kept at 4 °C while preliminary analysis was performed (Table 1). Paper was obtained from the office mix paper waste at Cranfield University and shredded to 3 × 10 mm before being used (Table 1).

2.2. Semi-continuous ADs and operational conditions

Three 20 l pilot scale digesters were operated, each of them inoculated with 15 kg of digestate at the start of the trials. Digesters were fed

Table 1
Digestate, OFMSW and paper characteristics.

Material	TS (%)	VS (%)	VS/TS (%)	C/N
Digestate	43.3 ± 3.4	13.1 ± 0.8	30.1 ± 3.9	15.9 ± 3.6
OFMSW	47.8 ± 2.5	28.4 ± 1.9	59.7 ± 6.5	16.2 ± 1.1
Paper	95.2 ± 0.4	80.7 ± 0.4	84.8 ± 0.5	329.4 ± 0.3

three times a week with a 1 to 3 ratio in mass of fresh feedstock and digestate extracted from the reactors. Excess digestate was removed to maintain a constant working weight inside the reactors and used for further analysis. The flow of biogas generated from each digester was measured with a CJC-125 gas counter and recorded in a CJC-034 data acquisition system (CJC Labs, Cumbria, UK). The reactors had no internal mixing and were maintained at mesophilic conditions (38 °C) in a Binder FP720 incubator (Binder GmbH, Tuttlingen, Germany).

Three different feedstocks were used in each of the digesters, reducing RT and increasing OLR to levels where instability was forced. One was fed solely with the OFMSW (ADW) for 145 days, which had a C/N of 16.2 ± 1.1. For the first 130 days of the trial the ADW reactor was operated with a 40-day RT (Table 2), equivalent to 6.5 ± 0.9 Kg VS/m^3/d, with a 2 week gap of no feed due to Covid-19 isolation of the author. The RT was reduced to 33 days from day 131, OLR of 7.5 ± 1.0 Kg VS/m^3/d, in order to stress the digester and highlight the inhibition mechanisms. The other two digesters were fed with a mixture of OFMSW and 15 % (AD15) or 20 % (AD20) of paper to increase C/N to 25 and 29, respectively. These values are in the range considered as optimum to avoid ammonia accumulation for wet AD (Bouallagui et al., 2009), as values in dry AD are not available in literature. The starting retention time for the first 69 days of digestion was kept at 40 days, which was reduced to 33 days until day 90 when the digesters were stopped (Table 2).

2.3. Analytical methods

Standard methods (APHA, 1999) were used to measure TS and VS of both feedstock and digestate. To analyse the rest of parameters the digestate was diluted following a similar methodology to Guendouz et al. (2010). One part of digestate was diluted with five parts of water and mixed in an orbital shaker (Cole-Palmer, St. Neots, UK) at room temperature for 30 min before centrifuging it in a Megafuge 16R centrifuge (Thermo Scientific, Massachusetts, USA) for 20 min at 4696 g and 4 °C. The supernatant was then used for the rest of analysis. pH was measured with a HQ440D Hatch multi-meter (HACH LANGE ltd, Manchester, UK) and alkalinity and Ripley ratio (RR) were obtained by titration until pH 5.7 and 4 (Ripley et al., 1997). Analysis of TAN and VFA were showed as conducted on the solids free fraction of the samples, which was obtained by filtering the supernatant through a 0.45 μm retention membrane filter (Whatman, Kent, UK). The analysis of VFA was performed with a Shimadzu VP Series HPLC unit (Milton Keynes, UK) with a 90 min run time using the methodology described in Rocamora et al. (2022b). Ion chromatography in a ICS900 (Dionex, California, USA) was used for TAN analysis with an IonPac CS12A as column and precolumn. A 20 mM methanesulphonic acid was used as eluent and 100 mM tetrabutylammonium hydroxide as regenerant. An injection volume of 20 μl with a 1 ml/min flow and ambient temperature was used for the analysis. FA was calculated using Davis equation to account for temperature, pH and ionic strength (Capson-Tojo et al., 2020). All values were calculated by litre of water in the digestate.

Biogas was analysed for methane, hydrogen and hydrogen sulphide content in a 990 Micro GC System (Agilent, California, USA) with 2 columns operated at 110 °C and 30 PSI. One was a MS5A SS with helium as carrier gas for hydrogen detection and the second one a PoraPLOT Q UM with argon as carrier gas for methane and hydrogen sulphide detection. Injection was done for 50 ms and 110 s was used as retention time. Methane flowrates are showed as litres by kilogram of VS fed and day. Additionally, biogas was tested for carbon isotope ratios of methane ($\delta^{13}C_{CH4}$) and carbon dioxide ($\delta^{13}C_{CO2}$) by continuous flow-isotope ratio mass spectrometry in a HP 6890 N gas chromatograph (Agilent, Santa Clara, CA), as described by Keppler et al. (2010). The dominant methanogenic pathway was determined by calculation of the apparent fractionation factor (α_c), as described in equation 1 (Whiticar et al., 1986; Whiticar, 1999):

$$\propto_c = \frac{\delta^{13}C_{CO_2} + 1000}{\delta^{13}C_{CH_4} + 1000} \quad (1)$$

Where $\alpha_c > 1.065$ corresponds to CO_2 dependent (hydrogenotrophic) methanogenesis, $\alpha_c < 1.055$ to acetate dependent methanogenesis, and hybrid production when α_c is between those values.

Digestate extracted from each reactor and biogas were analysed 3 times a week, and weekly moving averages were used to eliminate the impact of the feeding pattern in the results. Hydrogen concentrations on the headspace were determined with gas chromatography and partial pressures were calculated considering a pressure of 1 atm as headspace pressure. A higher partial pressure of hydrogen on the digesting broth than that of the headspace is expected, due to the reduced diffusion at high TS resulting in supersaturation on the broth (Bollon et al., 2013; Cazier et al., 2015).

2.4. Microbial analysis

Aliquots were taken periodically from the digestate extracted from the 3 pilot digesters (ADW, AD15 and AD20) and stored at −20 °C until analysis. The DNeasy PowerSoil Pro (Qiagen, UK) was used for DNA extraction according to manufacturer's protocol. The universal primers 515F – 806R targeting both bacteria and archaea were used for amplification of the V4 region of the 16S gene (Kozich et al., 2013). Illumina MiSeq platform (Illumina, USA) was used for 16S rRNA amplicon sequencing. QIIME 2 was used for raw data analysis and ASVs were generated according to DAD2 pipeline (Callahan et al., 2016) using RStudio version 4.0.3 (R Core Team, 2020) as described in Rocamora et al. (2022a) to obtain the relative presence of each microorganism in the digester, as this method is no capable of measuring activity. Statistical analyses of the microbial community presence were performed using Primer v7 (Clarke and Gorley, 2015) with PERMANOVA + add on to explore relationships between community changes. The ASV derived from the 16 s rRNA amplicon data was log (N + 1) transformed to down-weight the most abundant genera. Next, dissimilarities were calculated with the S17 Bray–Curtis similarity coefficient. A principal coordinate ordination analysis (PCoA) was performed by plotting the dissimilarity values for each factor. A correlation was performed between each physicochemical constituent (predictor variables) within the reactor (RT, hydrogen partial pressure, H_2S, FA, propionic and butyric acids) and each community coordinate. Correlations with each component were deemed significant ($R^2 > 0.5$) and a vector biplot was overlaid to visualize the strength and direction of this correlation. Distance-based linear modelling (DBLM) was performed to determine the effect of the different operational factors on microbial communities variability (Boj et al., 2010).

Table 2
Retention time (RT) and organic loading rate (OLR) for each experiment, with relative contribution from OFMSW and paper.

Digester	Time (days)	RT (days)	OLR (Kg VS/m^3/d)	OLR Waste (Kg VS/m^3/d)	OLR paper (Kg VS/m^3/d)
ADW	0–130	40	6.5 ± 0.9	6.5 ± 0.9	–
	131–145	33	7.5 ± 1.0	7.5 ± 1.0	–
AD15	0–69	40	7.3 ± 0.2	4.1 ± 0.1	3.2 ± 0.1
	69–90	33	8.3 ± 0.5	4.7 ± 0.4	3.6 ± 0.1
AD20	0–69	40	7.5 ± 0.2	3.4 ± 0.1	4.1 ± 0.1
	69–90	33	8.7 ± 0.4	3.9 ± 0.3	4.8 ± 0.1

3. Results and discussion

3.1. Mechanisms of inhibition and digester performance at high ammonia contents at C/N of 16 when digesting OFMSW alone

Methane production increased steadily in the start-up period until

80.6 ± 0.2 l CH_4/kg VS/d before the feeding was stopped on day 47, with the maximum daily methane production recorded on day 40 of operation at a value of 85.1 ± 1.3 l CH_4/kg VS/day (Fig. 1a). Methane flowrate decreased due to lack of feeding to 45.1 ± 1.2 l CH_4/kg VS/d on day 61. When feeding was re-started production increased to 71.6 ± 7.4 l CH_4/kg VS/d on day 96, after that the daily production decreased to 52.6 ± 0.4 l CH_4/kg VS/d on day 131 before the RT was reduced to 33 days. The RT reduction produced a faster decrease in methane production due to the increased inhibition, with a final daily methane production of 27.0 ± 0.5 l CH_4/kg VS/d on the last day of the experiment (day 145).

The feeding pattern impacted on the levels of the hydrogen partial pressure, with higher values measured at the end of the week due to weekly feeding. The hydrogen value recorded on the headspace on day 2

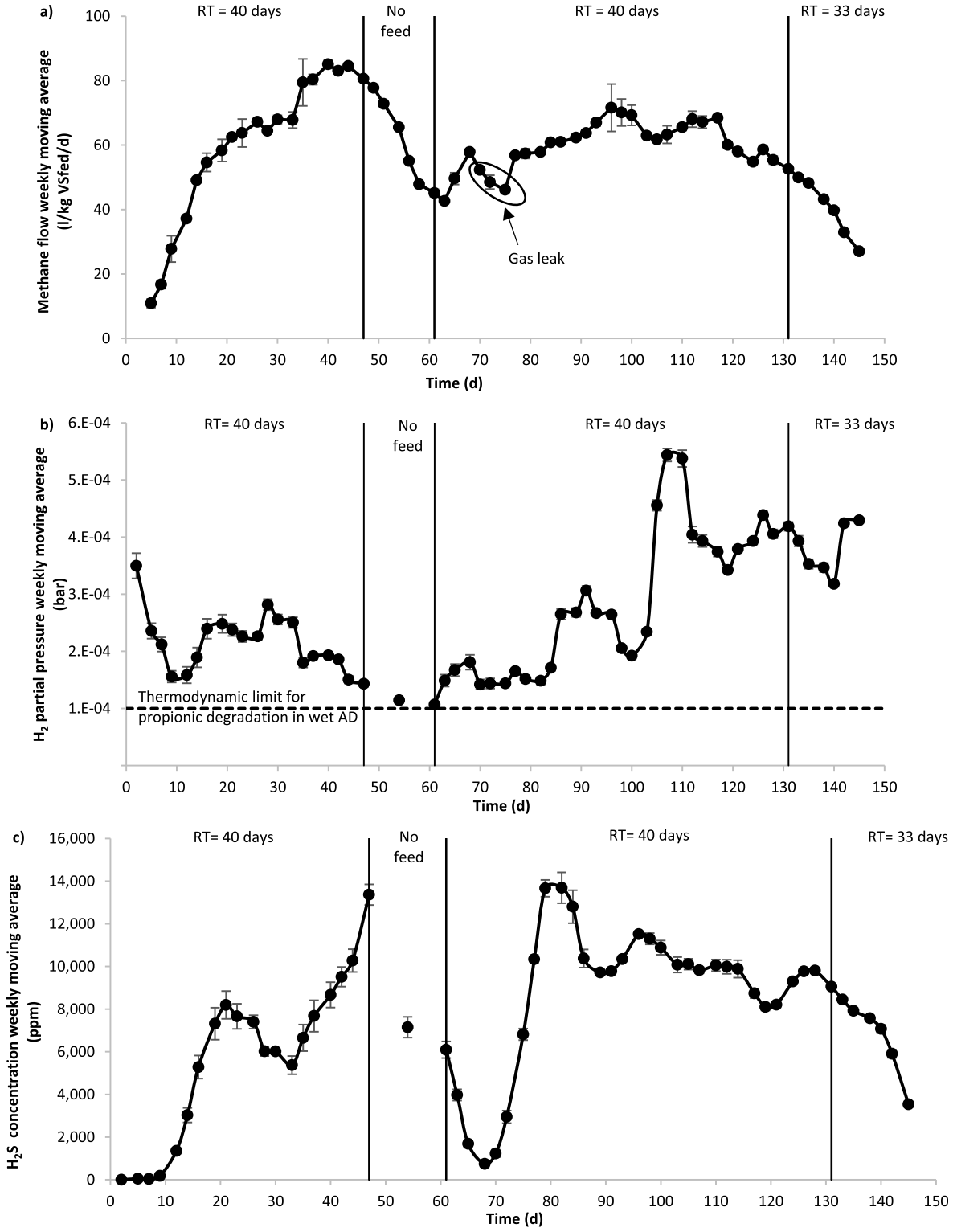

Fig. 1. Values of a) methane flow, b) hydrogen partial pressure, c) hydrogen sulphide concentration d) TAN and FA concentration and e) VFA for the digester fed with OFMSW only (ADW).

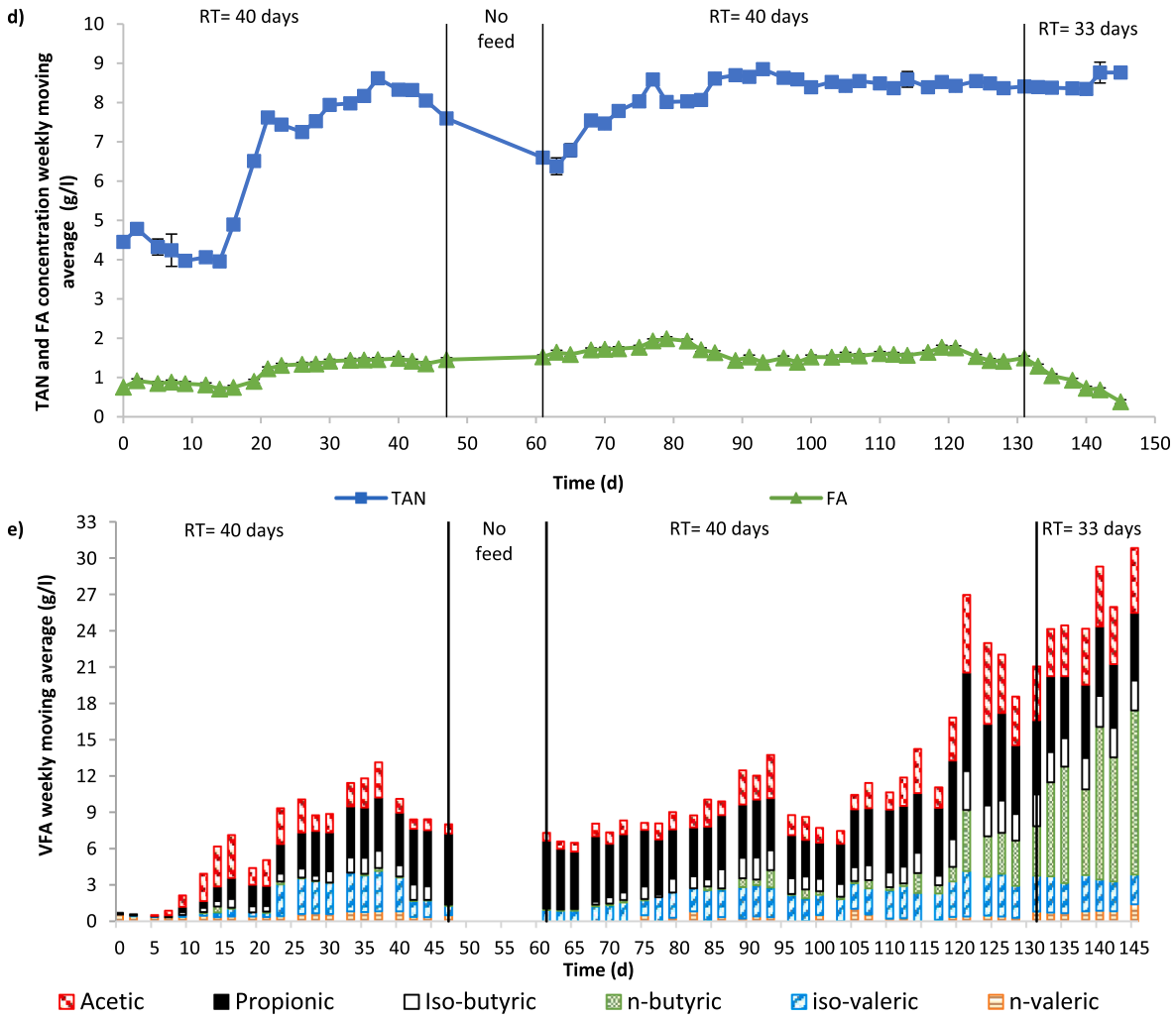

Fig. 1. (*continued*).

was 3.5×10^{-4} bar (Fig. 1b). This is a possible sign of inhibition, as values over 10^{-4} bar have been reported as the thermodynamic barrier for propionic decomposition in wet AD (Gujer and Zehnder, 1983) and values in the digesting broth are expected to be even higher due to the reduced diffusion. Hydrogen partial pressure varied between 1.4×10^{-4} bar and 3.1×10^{-4} bar between day 10 and 100. A big increase was recorded between days 107 and 110, with values over 5×10^{-4} bar. Hydrogen values dropped to 4.2×10^{-4} bar on day 131, before RT was reduced to 33 days. At the shorter RT an erratic trend was also observed, with lower values of 3.2×10^{-4} bar recorded on day 140 and a big increase to over 4×10^{-4} bar at the end of the experiment. The hydrogen sulphide profile followed a similar pattern to methane production (Fig. 1c), with an increasing trend from the onset of the trials until the feeding was stopped on day 47. After the feeding was re-started on day 61 hydrogen sulphide kept dropping for a week, then increased to a maximum of $13.7 \pm 0.7 \times 10^{3}$ ppm on day 82 and followed a decreasing trend until the end of the experiment. The RT shortening (and OLR increase) accelerated this decline, with a recording of $3.5 \pm 0.1 \times 10^{3}$ ppm on day 145 when the trial was stopped.

Initially TAN values were over 4 g/l in the digestate, and accumulation was observed from the beginning of the trial with values increasing until a plateau between 8.0 and 8.9 g/l (Fig. 1d). The initial FA in the digestate was 751 mg/l and followed a similar trend than TAN increasing until concentrations between 1.5 and 2.0 g/l (Fig. 1d). Propionic acid concentration in the digestate started at 40 mg/l, increasing to 445 mg/l on day 9 of operation when hydrogen partial pressure was 1.6×10^{-4} bar in the headspace. Hydrogen partial pressure was well over 10^{-4} bar in the headspace from the start, and the partial pressure in the digesting broth is expected to be even higher due to the reduced diffusion, which does not allow to conclude if higher values of hydrogen partial pressure are necessary to inhibit propionic degradation (Eq. 3) in dry AD than in wet AD. Propionic acid kept increasing to reach 5.9 g/l on day 47 and then decrease with time to 3.0 g/l by day 100. Values increased to a maximum of 8.1 g/l at day 121, oscillating between 5.1 and 6.2 g/l for the rest of the experiment regardless of the RT reduction.

An accumulation of *n*-butyric acid was also registered, with an increase on day 89 to 730 mg/l in parallel to an increase in hydrogen partial pressure to 2.7×10^{-4} bar in the headspace. From day 90 onwards *n*-butyric became the predominant VFA, reaching 13.5 g/l at the end of the experiment, when the digester was stopped due to the high instability and the decreasing methane production.

Hydrogen accumulation in the digester could be explained by an inhibition of hydrogenotrophic archaea resulting from the high FA. This inhibition would reduce hydrogen consumption by the archaea, reducing methane production and increasing hydrogen partial pressure in the system (Eq. 2). Propionic accumulation would then take place as its degradation by SPOB is thermodynamically hindered when hydrogen accumulates (Leng et al., 2018; Stams and Plugge, 2009). *N*-butyric accumulation would have followed a similar mechanism, but in this case, degradation would have been inhibited at a higher hydrogen partial pressure than propionic. The 2.7×10^{-4} bar recorded in the headspace is lower than 10^{-3} bar reported in literature (Harper and

Pohland, 1986), which could be explained by the higher hydrogen partial pressure in the digesting broth caused by the reduced diffusion (Bollon et al., 2013; Cazier et al., 2015). Acetic acid accumulation increased sharply when hydrogen partial pressure increased over 2.7 × 10^{-4} bar (Fig. 1b and 1e). It was hypothesized that the observed inhibition of SAOB together with an increase of the more thermodynamically favoured homoacetogenesis (Eq. 4) (Amani et al., 2010) could be responsible for the increase of acetic acid.

$$2CO_2 + 4H_2 \leftrightarrows CH_3COO^- + H^+ + 2H_2O \quad (4)$$

These results showed that hydrogen production in dry AD can be linked to organic overload due to the high OLR leading to VFA accumulation. These can lead to instability and even system failure, showing hydrogen monitoring as an interesting tool to control AD performance.

3.1.1. Microbial analysis

DBLM was performed to correlate RT, hydrogen partial pressure, H_2S, FA, propionate and butyric acids with microbial components of the reactor with the prokaryotic (bacteria) and archaea considered separately. The DBLM marginal tests revealed that the RT was the most important factor, governing 42 % and 38 % of the variability in bacteria and archaea communities respectfully (Supplementary table 1a & 2a), which confirms its importance in shaping the microbial communities in ADW. Butyric acid, propionic acid and hydrogen were the most important factors after accounting for RT for bacteria in ADW with 41 %, 28 % and 22 %, probably due its inhibitory effect. When archaea were analysed butyric acid, propionic acid and FA were in order the most important after RT being responsible for 30 %, 24 % and 20 % of the variability, showing the sensitivity of archaea to FA. During sequential testing the aim was to establish whether other predictor variables add a significant amount to the explained variation, given that RT has already been included in the model. For each model, the overall R^2 was 78 % and 73 % of bacterial and archaeal communities (Supplementary table 1b & 2b). In this case hydrogen sulphide and FA contributed to 14 % and 7 % ($p < 0.05$) of the variability and were the most important factors for bacteria, while hydrogen sulphide was the only significant variable for archaea with 13 % of contribution. Interestingly, all the analyses highlighted the RT as principal influence in shaping microbial communities, but also highlighted the important impact of butyric, which was accumulated at the end of the experiment, causing failure of the system. Propionic accumulation and hydrogen sulphide were both potent inhibitors of both the archaea and bacteria communities, but interestingly only the bacteria communities were significantly influenced by hydrogen ($p < 0.05$). This indicates an accumulation of hydrogen as predominantly inhibiting bacteria, especially SAB and SAOB, which in turn would cause the accumulation of propionic acid. The influence of FA was reduced compared to other variables and could probably be explained by the high FA present at the start of the digestion. These values were above inhibitory levels for acetogenic and hydrogenotrophic archaea (Jiang et al., 2019), which could indicate a previous selection of the microbial communities before the start of the digestion, reducing FA influence in the modelling.

Additionally, the representation of the communities via PCoA (Fig. 2a & b) visualised the RT influence on both bacteria and archaea communities. Three different periods could be distinguished by their microbial community's similarity, especially for archaea. Days 2 to 19, which could be considered the start-up period. Days 19 to 110, where methane production remained still relatively stable (Fig. 1a) and hydrogen exposed an increasing trend until the maximum values in the experiment (Fig. 1b). Days 121 to 145 matched the period with decreasing methane production (Fig. 1a) and accumulation of butyric acid (Fig. 1b), both signs of the inhibitory problems leading to reactor failure.

An enrichment in the genus *Anaerococcus* belonging to the *Firmicutes* phyla was observed at bacteria level during the reactor operation when the evolution of the most abundant phyla was studied (Fig. 3a and

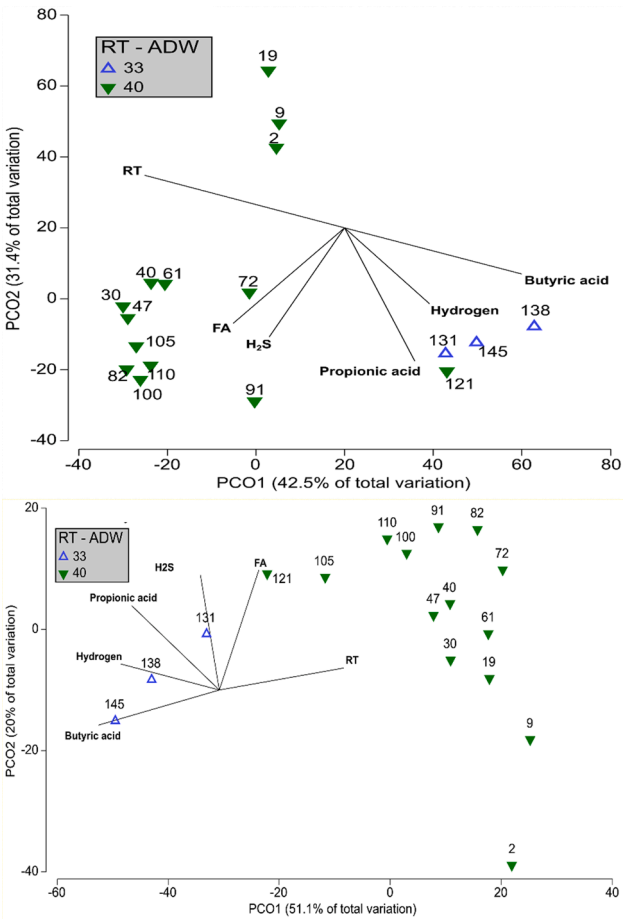

Fig. 2. Principal Coordinates Analysis for a) archaea and b) bacteria in ADW.

Supplementary Fig. 1a). Species in this genus contain genes for carbohydrate, amino acid and lipid metabolism (Tidjani Alou et al., 2016), which could be linked to the composition of OFMSW, rich in proteins. Due to the high TAN and FA contents in the inoculum *Methanosarcina* and *Methanoculleus* were predominant in the archaea analysis (Fig. 3b and Supplementary Fig. 1b), both known to tolerate TAN concentrations over 4 g/l (Bayrakdar et al., 2017; Vrieze et al., 2012; Yan et al., 2022), as was the case during all the digestion process. *Methanoculleus* is known to be a hydrogenotrophic methanogen (Fotidis et al., 2014b; Ollivier et al., 1986), found previously in dry AD (Bayrakdar et al., 2017; Li et al., 2014) and it also correlates with VFA increases (Dang et al., 2017; Franke-Whittle et al., 2014). *Methanosarcina* is a versatile methanogen, able to produce methane by both hydrogenotrophic and acetoclastic pathways (Liu and Whitman, 2008).

Methanosarcina relative abundance increased in ADW to become the most predominant methanogen at the end of the experiment, with values from 89.9 % to 100 % of the archaeal relative abundance since the RT was reduced to 33 days (Fig. 3b). This prevalence could be explained by their ability to form thick clumps and reduce diffusion of inhibitors, being easier for them to adapt to severe conditions such as unstable periods of anaerobic digestion (Bajón Fernández et al., 2019; Demirer and Chen, 2008), as it was the case in ADW due to the high FA and VFA concentrations in the digestating broth. It is also remarkable the loss of *Syntrophaceticus*, a SAOB, at similar times than *Methanoculleus*, suggesting a syntrophic relation between the two. This would agree with the previously mentioned mechanisms, as the loss of *Methanoculleus* in the ADs would lead to an accumulation of hydrogen followed by the inhibition and disappearance of *Syntrophaceticus*. Additionally, the modelling also highlights the importance of hydrogen on shaping bacterial communities but not archaeal communities.

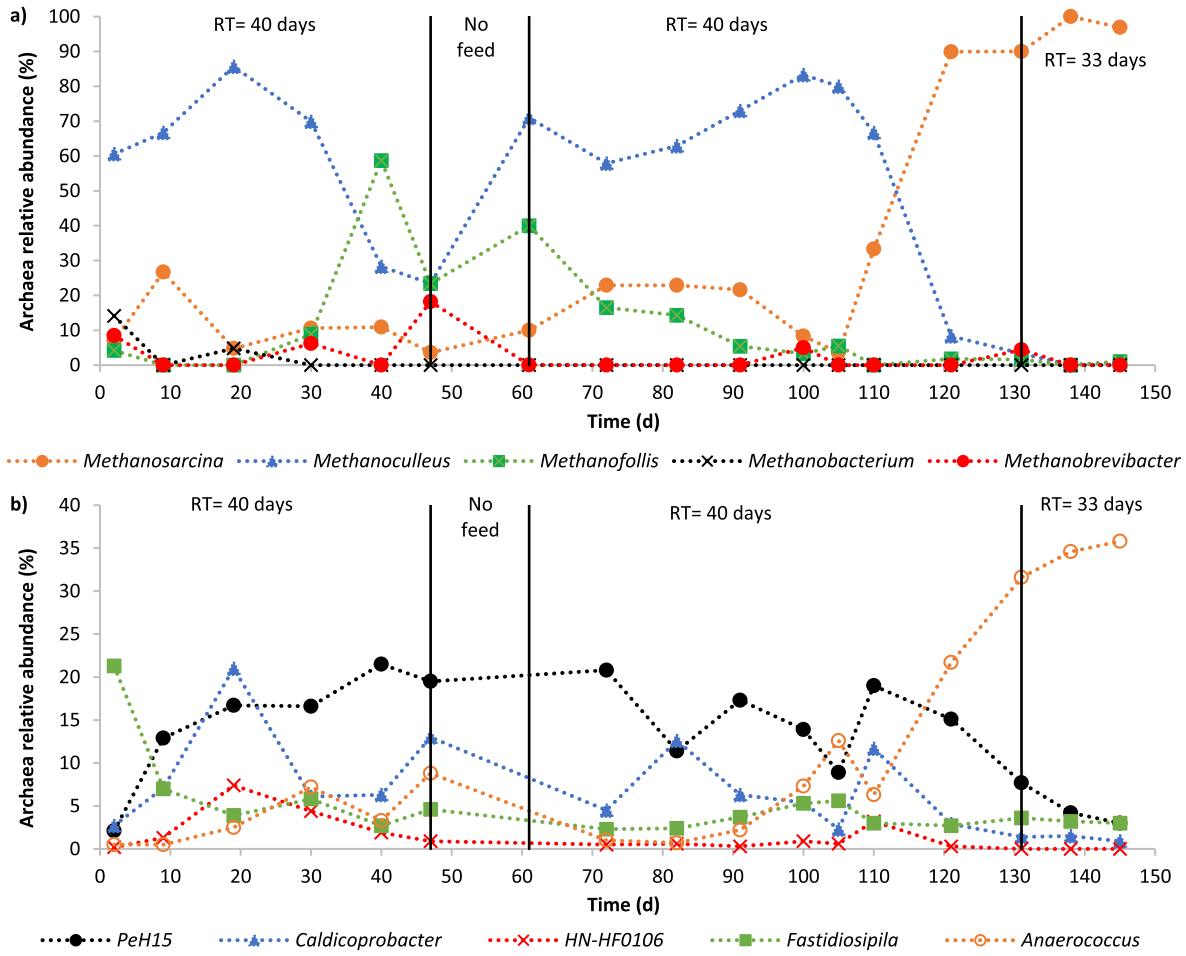

Fig. 3. Time-series of 5 most abundant a) bacteria and b) archaea on ADW.

Recorded values for carbon isotopic signature indicated a shift towards acetogenic methane production when FA concentrations remained between 1.2 and 2.0 g/l (Fig. 4). These values bring further knowledge to current literature, as it is reported that hydrogenotrophic methanogenesis is predominant at high TAN (>4 g/l) and FA (>200 mg/l) (Calli et al., 2005; Jiang et al., 2018; Westerholm et al., 2012). This change in methanogenic pathway occurred when an SAOB like *Syntrophaceticus* started to decrease its relative abundance and *Methanosarcina* became the predominant methanogen from day 121, coinciding with the third period (days 121 to 145) identified in the principal coordinates analysis (PCoA) (Fig. 2a & b). A hypothesis that could explain this phenomenon is that the inhibition of the SAOB increased its doubling time and resulted in its wash out, which stopped the oxidation of acetate to carbon dioxide and hydrogen for hydrogenotrophs use. Acetic acid was then used in the acetoclastic pathway, where *Methanosarcina* converted it to methane. It is possible to hypothesize that the long doubling

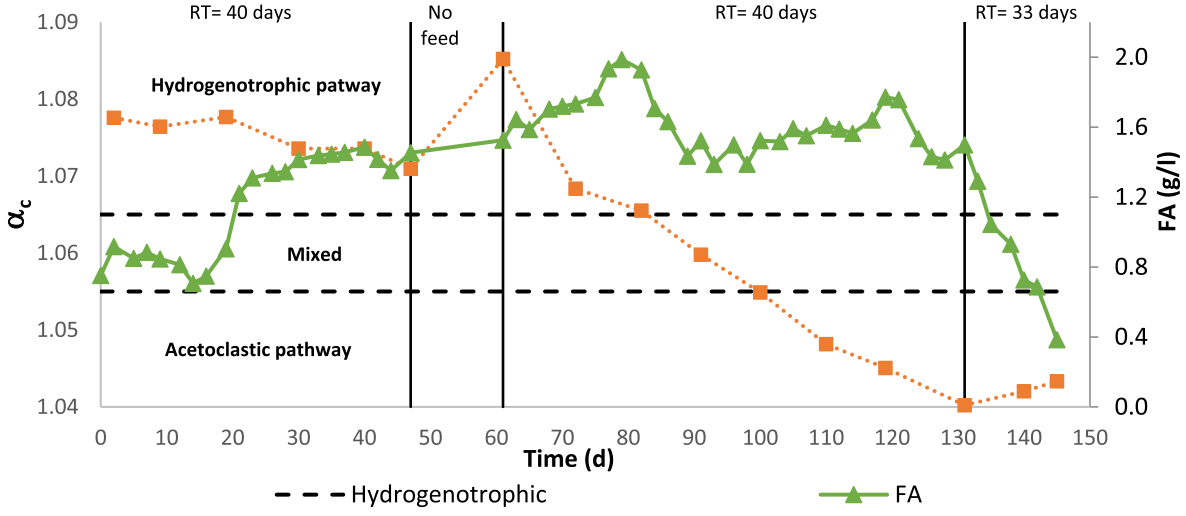

Fig. 4. Isotopic fractionation factor and FA profiles for ADW.

time of SAOB could be responsible for this shift, and probably the reason for the importance of the RT in shaping the microbial communities highlighted by PCoA. Doubling time has been reported to take up to 28 days for SAOB at TAN of 8 g/l and pH over 7 (Schnürer et al., 1999). It is reasonable to hypothesise that the increased pH of the digesters over 8 and the high TS could be affecting this doubling time, and higher RT than 40 days would be needed to achieve stable conditions. However, this would need further confirmation with tests on doubling rates at different environmental conditions. As an example, Schnürer and Nordberg (2008) reported stable operation with syntrophic acetate oxidation as the dominating pathway from acetate at 56-day RT, pH of 8 and TAN of 5.3 g/l in a full-scale plant. Fotidis et al. (2013) also found acetoclastic methanogenesis and *Methanosarcina* as dominant when TAN was 7 g/l. Sodium acetate was used as substrate in successive batch AD with acclimatised cultures to TAN increasing concentration from 1 to 7 g/l. The authors postulated a hypothesis were acetic was used by

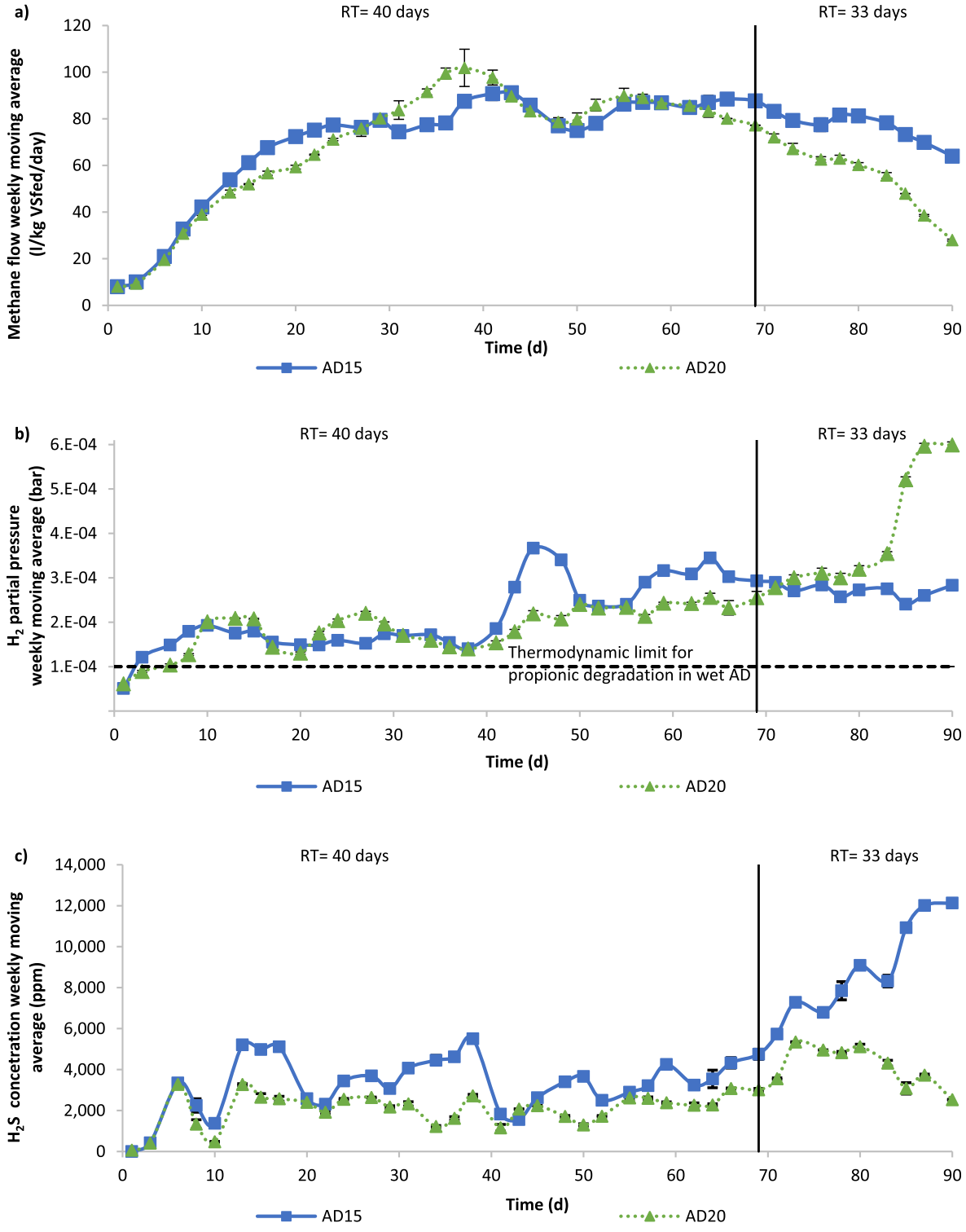

Fig. 5. Values of a) methane flow, b) hydrogen partial pressure, c) hydrogen sulphide concentration, d) TAN and FA concentration for AD15 and AD20 and VFA profile for e) AD15 and f) AD20.

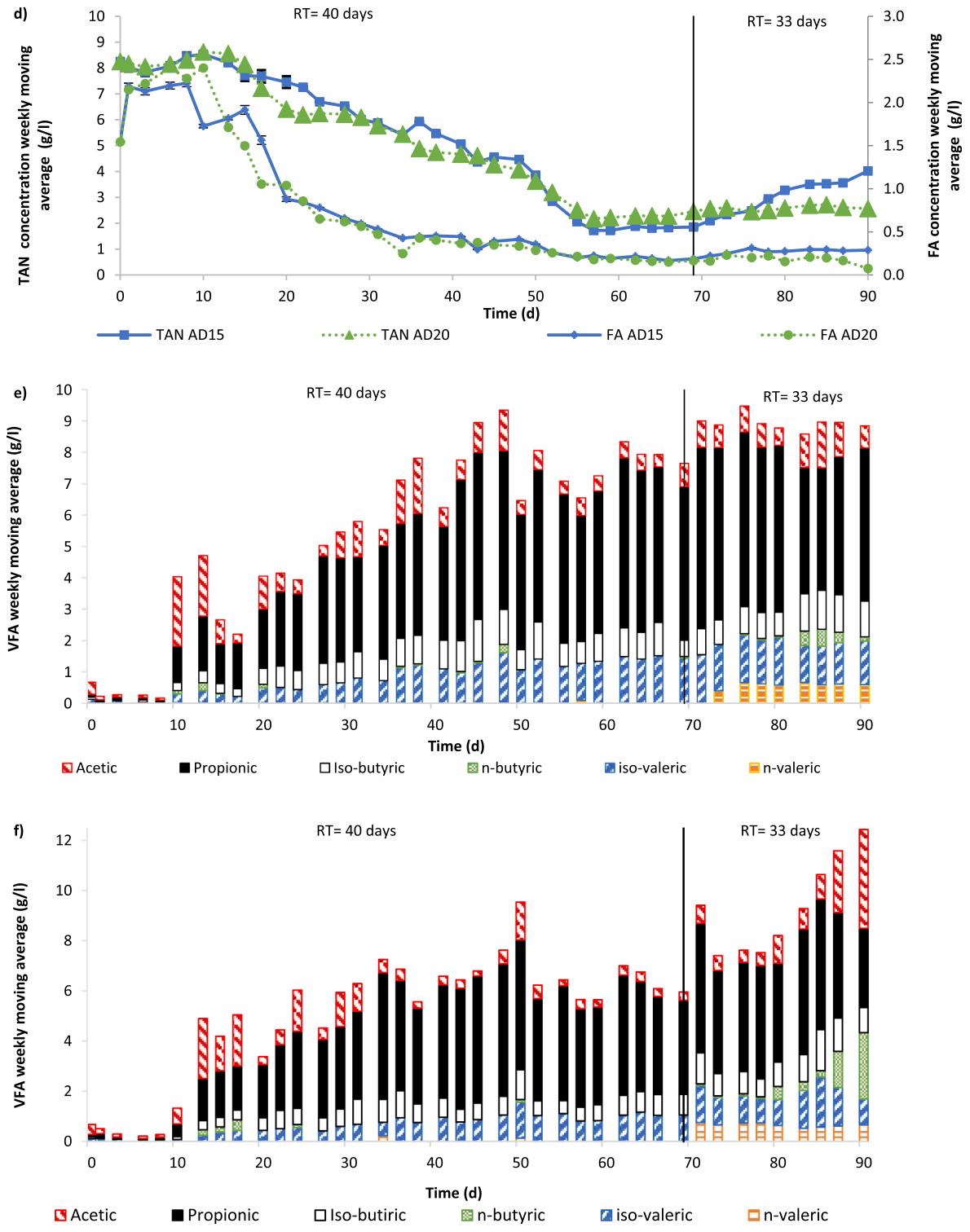

Fig. 5. (*continued*).

Methanosarcina due to the inhibition of the SAOB. However, results were different when cultures were not acclimatised, as hydrogenotrophic methanogenesis was dominant and hydrogenotrophs, other than *Methanosarcina,* were present. These results could be explained with the hypothesis of insufficient doubling time for SAOB when cultures were acclimatised. The digestion time would not have been enough for syntrophic bacteria to grow when inoculum from the previous batch was used to inoculate the next batch, leaving *Methanosarcina* and acetoclastic methanogenesis as dominants.

3.2. Inhibition mechanisms and digester performance at increased C/N

The highest daily methane production (Fig. 5a) per kg of VS fed was achieved by AD20 with 105 ± 2 l CH_4/kg VS/d, while AD15 achieved 97 ± 2 l CH_4/kg VS/d, both higher than ADW but without a statistically significant difference ($p > 0.05$). Hydrogen partial pressure remained lower than for ADW in both AD15 and AD20 (Fig. 4b), which together with the higher methane production could indicate a lower inhibition. The thermodynamic limit of 10^{-4} bar reported for wet AD for propionic

acid degradation was surpassed on day 6 for AD15, while it took until day 9 on AD20. This delay could be linked to a reduced inhibition due to the higher C/N ratio, as ammonia accumulation was reduced from the initial 8 g/l to<3 g/l in both ADs. Hydrogen partial pressure in AD15 peaked at 3.7×10^{-4} bar on day 45, which could be correlated to a drop in methane production during these days, suggesting inhibition of the methanogens. After that day values ranged between 3.4×10^{-4} bar and 2.4×10^{-4} bar until the end of the experiment. Hydrogen partial pressure in AD20 increased steadily during the first 69 days of operation (40-day RT), reaching a maximum value of 2.6×10^{-4} bar before the RT reduction. From this point onwards partial pressure increased at a higher rate, which turned into an exponential increment from day 85 until the end of the trial when values reached 6.0×10^{-4} bar. This raise was a sign of the increasing inhibition of the hydrogenotrophic archaea, confirmed by the fast decrease on methane production.

Hydrogen sulphide concentration remained at lower values than those in ADW due to the C/N increase, which could be linked to the reduction of proteins in the feed, main source for sulphur (Tian et al., 2020). Concentrations of hydrogen sulphide in both AD15 and AD20 increased along the digestion period, with a rise in AD15 after RT was reduced to 33 days, however concentrations in AD20 started to decrease after day 80.

Initial TAN values were at 8 g/l and were reduced with time in both AD15 and AD20. The concentration in AD15 was reduced to 2.2 g/l on day 69 and increased steadily up to 4 g/l after the RT was reduced to 33 days. In AD20 the TAN level was reduced to 2.5 g/l before RT was decreased to 33 days, remaining around this value until the end of the trial. FA started with values over 1.5 g/l for both ADs, followed by an increase to 2.2 g/l on day 8 for AD15 and 2.4 g/l for AD20 on day 10. Both decreased steadily from that point reaching values under 100 mg/l at the end of the experiment. These results were expected, as the reduction on ammonia accumulation by increasing C/N ratio has been recorded previously in literature. As an example, Zeshan et al. (2012) reduced ammonia content in the digester by 30 % when increasing C/N from 27 to 32 using pilot scale thermophilic reactors co-digesting food, green and paper waste at 20 % TS.

Propionic accumulation followed a similar trend as for ADW, but this time started at day 10 for AD15 and AD20 (Fig. 4e and 4f). In this case, accumulation was lower, recording maximum values over 5 g/l for both AD15 and AD20, while ADW maximum values reached over 8 g/l. In both ADs propionic accumulation started when hydrogen partial pressure in the headspace reached 2×10^{-4} bar, higher than values in ADW. Only a small increase in *n*-butyric was registered on AD15 and was reduced to 150 mg/l before the digester was stopped, despite values of hydrogen partial pressure around 2.8×10^{-4} bar in the headspace being similar to the levels that triggered *n*-butyric accumulation in ADW. Meanwhile, AD20 registered a steep increase in acid accumulation from day 85, reaching 2.6 g/l of *n*-butyric and 3.9 g/l of acetic by the end of the experiment. This happened when the hydrogen partial pressure reached values over 3.5×10^{-4} bar, again higher than the values registered in ADW when *n*-butyric accumulation started. Results showed that an increase on C/N ratio improved methane production but was unable to avoid the ultimate failure of the system at the RT and OLR times tested. The increase of C/N from 16 to 25 (AD15) and 29 (AD20) reduced ammonia levels from 8 g/l to 2.2 and 2.5 g/l by the end of the digestion trial, and the maximum peak of propionic concentration was reduced by 29 and 37 % in AD15 and AD20, respectively. Propionic started to accumulate at 2.0×10^{-4} bar in AD20 and AD15, higher than the 1.6×10^{-4} bar in ADW. Additionally, *n*-butyric accumulation also occurred at a higher hydrogen partial pressure when C/N was increased, with accumulation in ADW after 2.7×10^{-4} bar compared to 3.5×10^{-4} bar in AD20. This could be linked to the TAN levels in the ADs, as values were over 8.6 g/l for ADW compared to 2.7 g/l in AD20. Interestingly, although hydrogen partial pressure was higher for AD15 and provoked higher propionic concentrations along most of the digestion time at 40-day RT, it was AD20 after the reduction of RT, which showed a higher instability with a steep increase in hydrogen production. This triggered *n*-butyric and acetic accumulation before the digesters were stopped. Additionally, production of hydrogen sulphide kept increasing until the end of the experiment and methane production remained higher in AD15 compared to AD20. This would suggest a lower inhibition in AD15 or differences on microbial communities. Furthermore, although methane flows were increased with the use of paper, it is necessary to account for the loss of throughput, and the use of paper will reduce OFMSW treatment capacity. Alternative strategies that can sustain methane production and process stability without significantly compromising treatment capacity merit further investigation. Some of these are the increase on direct interspecies electron transfer using biochar (Tsui et al., 2022), activated carbon (Xu et al., 2018) or other conductive materials (Dang et al., 2017); or the use of trace elements targeting an improved VFA degradation (Šafarič et al., 2020; Song et al., 2020).

3.3. Microbial analysis

When DBLM was performed for AD1, marginal tests revealed FA and propionic acid concentrations as the most important factors on impacting bacteria variability (Supplementary table 3), governing 50 % and 49 % of the variability. After accounting for the RT, hydrogen became the most important factor being responsible for 22 % of the variability, with a total R^2 of 80 % (Supplementary table 3b). The effect on archaea was different, and none of the factors in the DBLM were significant ($p > 0.05$) (Supplementary table 4a & b). When AD20 was analysed, FA and propionic acid levels were again the most important factors governing bacteria variability (Supplementary table 5a) with 52 % and 49 % percent respectively, and FA was the most important contributing to 23 % of the variability after accounting for the RT (Supplementary table 5b), similarly to AD15. Archaea variability in AD20 was explained mainly by FA, propionic and hydrogen sulphide which governed 81 %, 65 % and 38 % of the variability (Supplementary table 6a). When RT was controlled, only FA was significant ($p < 0.05$) being responsible for 42 % of the variability of the model, with a total of R^2 of 93 % (Supplementary table 6b). The analysis of both AD15 and AD20 evidenced a strong impact of propionic and specially FA on the variability of microbial communities, which was different than in ADW. The model showed that FA decrease with the digestion time in both AD15 and AD20 impacted more the microbial communities evolution than in ADW, where FA consistently remained at inhibitory levels even for hydrogenotrophic archaea (Jiang et al., 2019). Propionic importance was higher in AD15 and AD20 than in ADW, were butyric had higher impact. This could result from the lower levels of butyric found in the co-digestion digesters, where propionic remained the most dominant VFA, being one of the main causes for inhibition.

Bacteria in AD15 and AD20 appeared to be enriched in the family *PeH15* (Fig. 6a & c), corresponding to the phylum *Bacteroidales* and genus *HN-HF0106*, family *Hungateiclostridiaceae* and phylum *Firmicutes*. These results were linked to the addition of paper in the feed, as these phyla are related to the degradation of complex hydrocarbons, with *Bacteroidales* being common in digestion of lignocellulosic compounds (Sun et al., 2015) and the *Clostridiaceae* family being known to hydrolyse cellulose (Suksong et al., 2019).

Methanoculleus was the predominant methanogen in AD15 until day 20, when *Methanosarcina* became the dominant methanogenic archaea. The same increase on *Methanosarcina* relative abundance occurred from the beginning of the trial in AD20, probably resulting from the reduction of ammonia levels in both ADs (Fig. 6b & d). Additionally, the hydrogenotrophic archaea *Methanofollis* showed a consistent increase in AD15 and AD20 with the decline of *Methanoculleus*, which is more pronounced after the RT reduction to 33 d. *Methanofollis* is a hydrogenotrophic archaea that utilizes H_2/CO_2, formate, 2-propanol/CO_2, and 2-butanol/CO_2 for growth and methanogenesis (Imachi et al., 2009; Lai, 2019), which could be better adapted at lower TAN concentrations than

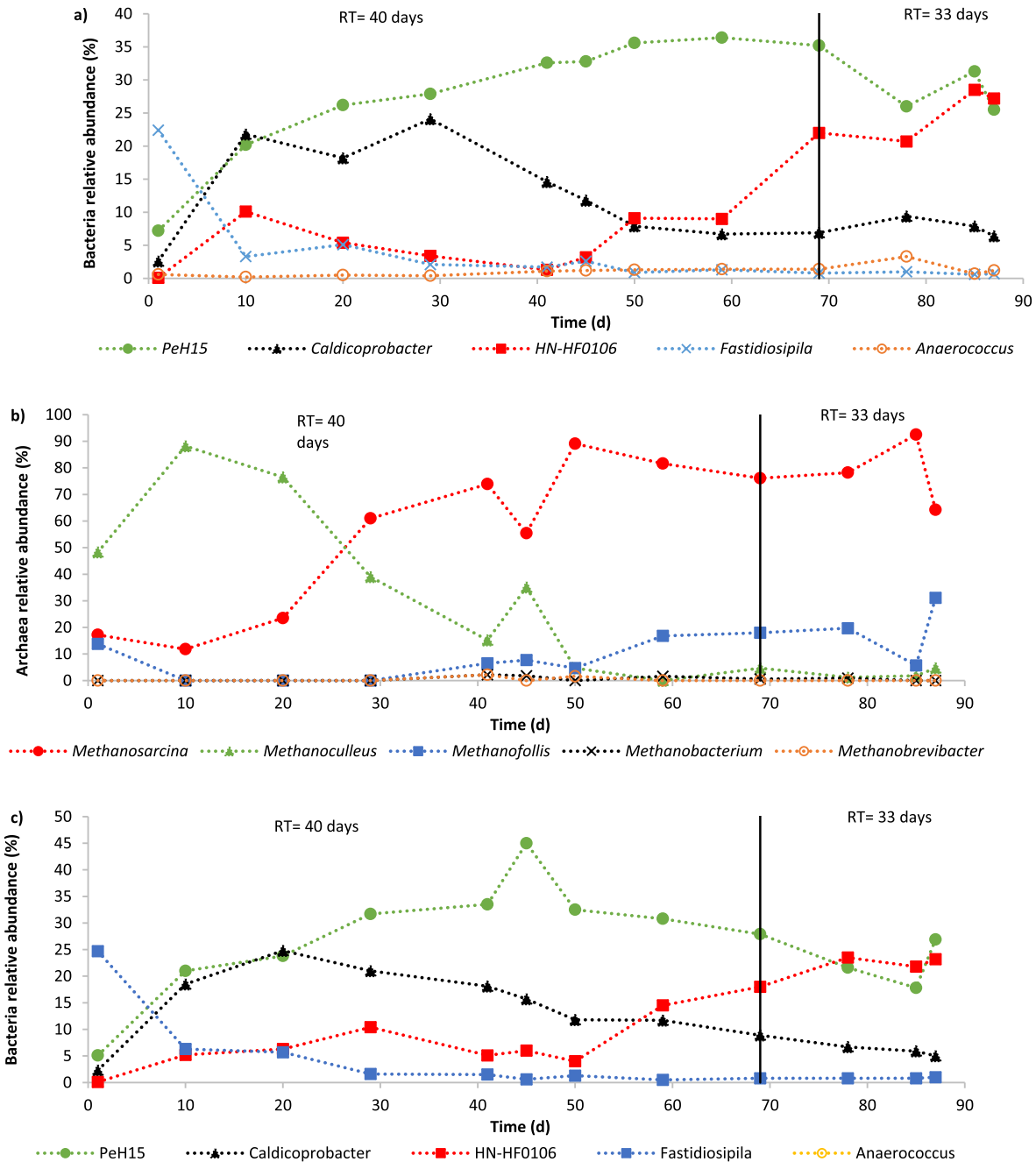

Fig. 6. Evolution of 5 most abundant a) bacteria and b) archaea in AD15 and c) bacteria and d) archaea in AD20 and isotopic fractionation factor and FA levels for e) AD15 and f) AD20.

Methanoculleus.

Similarly to ADW, the shift of the carbon isotopic signature towards acetoclastic methanogenesis (Fig. 6e & f) could be linked to a change in the methanogenic pathway by *Methanosarcina*, able to use both methanogenic pathways. Contrarily to ADW ammonia reduction occurred along the digestion period in AD15 and AD20, and it is possible to hypothesize that this could have been responsible for this shift. The pathway shift was recorded around day 69 for AD15 and day 59 for AD20, when both reached FA values under 200 mg/l, similar to values reported in literature for the shift in methanogenic pathways (Schnürer and Nordberg, 2008). However, *Syntrophaceticus* and *Methanoculleus* relative abundance started to decrease for both ADs at the same time, around day 50, shortly before the methanogen pathway was shifted to acetoclastic. This reduction was similar in ADW and could be explained by the washout of SAOB provoked by the long doubling time of SAOB, another factor helping *Methanosarcina* to become the dominant methanogen. For this reasons SAOB washout could also be responsible for the shift in methanogenic pathways like reported in ADW, and further work is necessary to clarify these mechanisms. Additionally, this study has limitations, as RT were deliberately short to force inhibition. Longer RT need to be assessed to gain further understanding on increasing C/N ratios using co-digestion with paper, especially on the effect on microbial communities. It is also necessary to analyse the effect of increasing TS, FA and VFA independently on SAOB doubling times to verify the hypothesis of the increased doubling times of SAOB with unfavourable conditions.

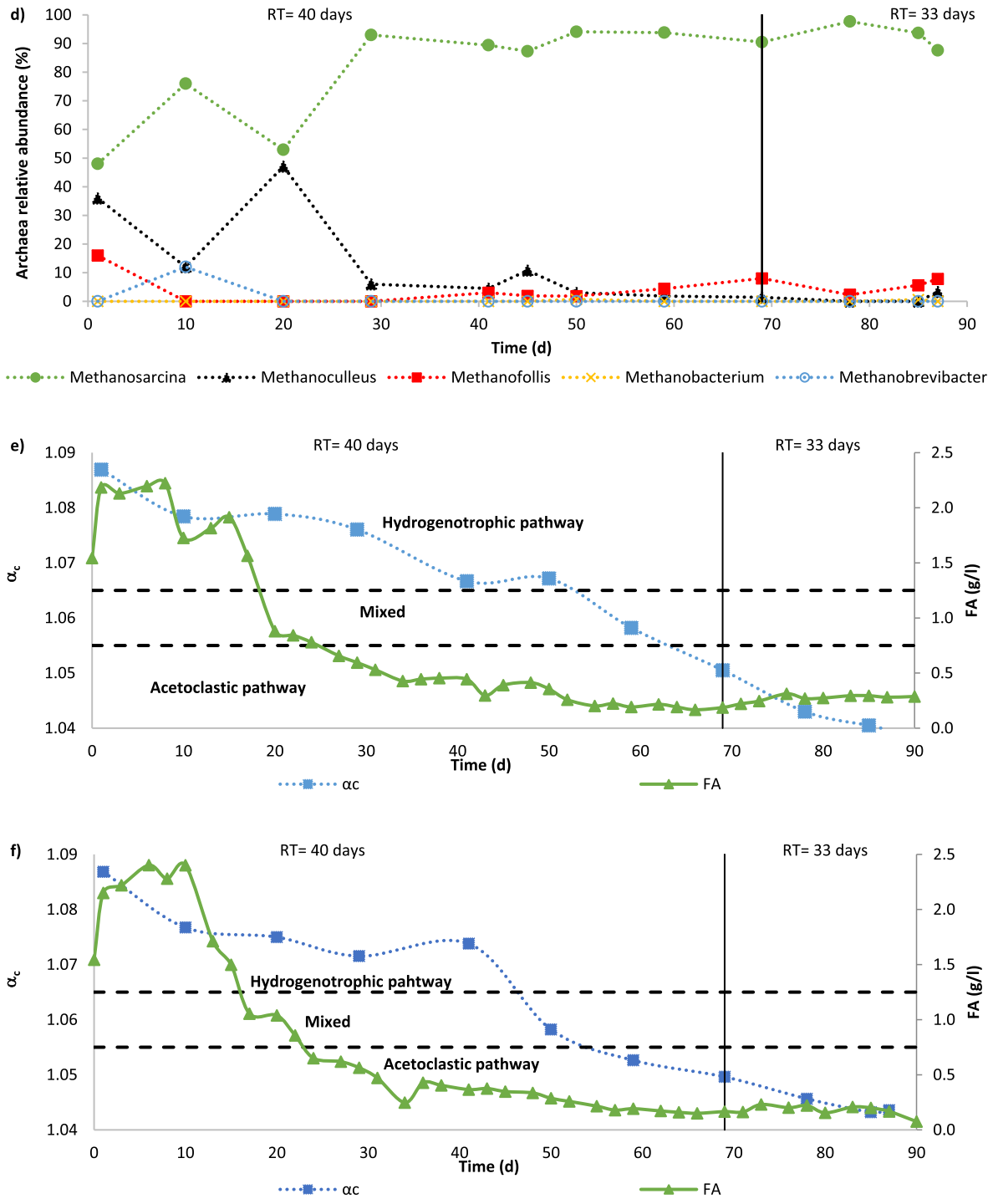

Fig. 6. (*continued*).

4. Conclusions and prospects

Previous literature investigating the inhibitory pathways of AD is limited to wet systems and dry AD up to 20 % TS, with a lack of knowledge for reactors with increased TS levels. The main novelty of this work is providing evidence of sustained acetoclastic methanogenesis at elevated ammonia levels in dry ADs, which has enabled an informed hypothesis on the mechanisms of inhibition of dry ADs to be postulated. It is hypothesised that inhibitory levels of FA on the digesting broth inhibited strict hydrogenotrophic methanogens, increasing H_2 partial pressure, leading to accumulation of propionic and *n*-butyric acids and impacting the doubling time of SAOB that were then washed out of the reactors and forced a shift to acetoclastic pathway of versatile methanogens. Paper co-digestion increased C/N ratio but did not avoid VFA accumulation despite resulting in a significant TAN reduction at the RT and OLR tested.

The insights of this study on mechanisms of inhibition of dry ADs provide a basis for further research on strategies to avoid inhibition, particularly focusing on stopping propionate and hydrogen accumulation in the process.

Data Availability

All relevant data are provided within the manuscript or as

supplementary material.

Declaration of Competing Interest

The authors declare that they have no known competing financial interests or personal relationships that could have appeared to influence the work reported in this paper.

Data availability

Data will be made available on request.

Acknowledgements

This work was undertaken during I. Rocamora's Engineering Doctorate research at Cranfield University, funded jointly by the Engineering & Physical Sciences Research Council (EPSRC) Skills Technology Research and Management (STREAM) EngD Programme (Grant EP/L015412/1) and Amey Waste Treatment.

M. Peces acknowledges the funding from the European Union's Horizon 2020 research and innovation programme under the Marie Sklodowska-Curie grant agreement 101023927.

Appendix A. Supplementary data

Supplementary data to this article can be found online at https://doi.org/10.1016/j.wasman.2023.02.009.

References

ADBA, 2021. Anaerobic Digestion Policy Report.
Ahring, B.K., Westermann, P., 1988. Product Inhibition of Butyrate Metabolism by Acetate and Hydrogen in a Thermophilic Coculture. Appl. Environ. Microbiol. 54, 2393–2397. https://doi.org/10.1128/aem.54.10.2393-2397.1988.
Amani, T., Nosrati, M., Sreekrishnan, T.R., 2010. Anaerobic digestion from the viewpoint of microbiological, chemical, and operational aspects — a review. Environ. Rev. 18, 255–278. https://doi.org/10.1139/A10-011.
Angelidaki, I., Ahring, B.K., 1993. Thermophilic anaerobic digestion of livestock waste: the effect of ammonia. Appl. Microbiol. Biotechnol. 38 https://doi.org/10.1007/BF00242955.
APHA, 1999. Standard Methods for Examination of Water and Wastewater., American Public Health Association, American Water Works Association and Water Environmental Federation: Washington, DC, USA. https://doi.org/ISBN 9780875532356.
Bajón Fernández, Y., Soares, A., Vale, P., Koch, K., Masse, A.L., Cartmell, E., 2019. Enhancing the anaerobic digestion process through carbon dioxide enrichment: initial insights into mechanisms of utilization. Environ. Technol. 40, 1744–1755. https://doi.org/10.1080/09593330.2019.1597173.
Banks, C.J., Zhang, Y., Jiang, Y., Heaven, S., 2012. Trace element requirements for stable food waste digestion at elevated ammonia concentrations. Bioresour. Technol. 104, 127–135. https://doi.org/10.1016/j.biortech.2011.10.068.
Bayrakdar, A., Sürmeli, R.Ö., Çalli, B., 2017. Dry anaerobic digestion of chicken manure coupled with membrane separation of ammonia. Bioresour. Technol. 244, 816–823. https://doi.org/10.1016/j.biortech.2017.08.047.
Boj, E., Delicado, P., Fortiana, J., 2010. Distance-based local linear regression for functional predictors. Comput. Stat. Data Anal. 54, 429–437. https://doi.org/10.1016/j.csda.2009.09.010.
Bollon, J., Benbelkacem, H., Gourdon, R., Buffière, P., 2013. Measurement of diffusion coefficients in dry anaerobic digestion media. Chem. Eng. Sci. 89, 115–119. https://doi.org/10.1016/j.ces.2012.11.036.
Bouallagui, H., Lahdheb, H., Ben Romdan, E., Rachdi, B., Hamdi, M., 2009. Improvement of fruit and vegetable waste anaerobic digestion performance and stability with co-substrates addition. J. Environ. Manage. 90, 1844–1849. https://doi.org/10.1016/j.jenvman.2008.12.002.
Callahan, B.J., McMurdie, P.J., Rosen, M.J., Han, A.W., Johnson, A.J.A., Holmes, S.P., 2016. DADA2: High-resolution sample inference from Illumina amplicon data. Nat. Methods 13, 581–583. https://doi.org/10.1038/nmeth.3869.
Calli, B., Mertoglu, B., Inanc, B., Yenigun, O., 2005. Effects of high free ammonia concentrations on the performances of anaerobic bioreactors. Process Biochem. 40, 1285–1292. https://doi.org/10.1016/j.procbio.2004.05.008.
Capson-tojo, G., Trably, E., Rouez, M., Crest, M., Steyer, J., Delgenès, J., Escudié, R., 2017. Dry anaerobic digestion of food waste and cardboard at different substrate loads, solid contents and co-digestion proportions. Bioresour. Technol. 233, 166–175. https://doi.org/10.1016/j.biortech.2017.02.126.
Capson-Tojo, G., Moscoviz, R., Astals, S., Robles, S., J.p.,, 2020. Unraveling the literature chaos around free ammonia inhibition in anaerobic digestion. Renew. Sustain. Energy Rev. 117, 109487 https://doi.org/10.1016/j.rser.2019.109487.
Cazier, E.A., Trably, E., Steyer, J.P., Escudie, R., 2015. Biomass hydrolysis inhibition at high hydrogen partial pressure in solid-state anaerobic digestion. Bioresour. Technol. 190, 106–113. https://doi.org/10.1016/j.biortech.2015.04.055.
Choong, Y.Y., Norli, I., Abdullah, A.Z., Yhaya, M.F., 2016. Impacts of trace element supplementation on the performance of anaerobic digestion process: A critical review. Bioresour. Technol. 209, 369–379. https://doi.org/10.1016/j.biortech.2016.03.028.
Clarke, K.R., Gorley, R.N., 2015. Primer: User manual/tutorial. Prim. Ltd., Plymouth, UK, p. 93.
Dang, Y., Sun, D., Woodard, T.L., Wang, L.Y., Nevin, K.P., Holmes, D.E., 2017. Stimulation of the anaerobic digestion of the dry organic fraction of municipal solid waste (OFMSW) with carbon-based conductive materials. Bioresour. Technol. 238, 30–38. https://doi.org/10.1016/j.biortech.2017.04.021.
Demirer, G.N., Chen, S., 2008. Anaerobic biogasification of undiluted dairy manure in leaching bed reactors. Waste Manag. 28, 112–119. https://doi.org/10.1016/j.wasman.2006.11.005.
Ec,, 2020. Long-term low greenhouse gas emission development strategy of the European Union and its Member States. Eur. Comm. 2019, 1–7.
EU, 2021. Food waste reduction targets – content of the inception impact assessment. EU Platform on Food Losses and Food Waste.
Fotidis, I.A., Karakashev, D., Kotsopoulos, T.A., Martzopoulos, G.G., Angelidaki, I., 2013. Effect of ammonium and acetate on methanogenic pathway and methanogenic community composition. FEMS Microbiol. Ecol. 83, 38–48. https://doi.org/10.1111/j.1574-6941.2012.01456.x.
Fotidis, I.A., Karakashev, D., Angelidaki, I., 2014a. The dominant acetate degradation pathway/methanogenic composition in full-scale anaerobic digesters operating under different ammonia levels. Int. J. Environ. Sci. Technol. 11, 2087–2094. https://doi.org/10.1007/s13762-013-0407-9.
Fotidis, I.A., Wang, H., Fiedel, N.R., Luo, G., Karakashev, D.B., Angelidaki, I., 2014b. Bioaugmentation as a Solution To Increase Methane Production from an Ammonia-Rich Substrate. Environ. Sci. Technol. 48, 7669–7676. https://doi.org/10.1021/es5017075.
Franke-Whittle, I.H., Walter, A., Ebner, C., Insam, H., 2014. Investigation into the effect of high concentrations of volatile fatty acids in anaerobic digestion on methanogenic communities. Waste Manag. 34, 2080–2089. https://doi.org/10.1016/j.wasman.2014.07.020.
Guendouz, J., Buffière, P., Cacho, J., Carrère, M., Delgenes, J.P., 2010. Dry anaerobic digestion in batch mode: Design and operation of a laboratory-scale, completely mixed reactor. Waste Manag. 30, 1768–1771. https://doi.org/10.1016/j.wasman.2009.12.024.
Gujer, W., Zehnder, A.J.B., 1983. Conversion processes in anaerobic digestion. Water Sci. Technol. 15, 127–167. https://doi.org/10.2166/wst.1983.0164.
Harper, S.R., Pohland, F.G., 1986. Recent developments in hydrogen management during anaerobic biological wastewater treatment. Biotechnol. Bioeng. 28, 585–602. https://doi.org/10.1002/bit.260280416.
Imachi, H., Sakai, S., Nagai, H., Yamaguchi, T., Takai, K., 2009. Methanofollis ethanolicus sp. nov., an ethanol-utilizing methanogen isolated from a lotus field. Int. J. Syst. Evol. Microbiol. 59, 800–805. https://doi.org/10.1099/ijs.0.003731-0.
Jiang, Y., Banks, C., Zhang, Y., Heaven, S., Longhurst, P., 2018. Quantifying the percentage of methane formation via acetoclastic and syntrophic acetate oxidation pathways in anaerobic digesters. Waste Manag. 71, 749–756. https://doi.org/10.1016/j.wasman.2017.04.005.
Jiang, Y., McAdam, E., Zhang, Y., Heaven, S., Banks, C., Longhurst, P., 2019. Ammonia inhibition and toxicity in anaerobic digestion: A critical review. J. Water Process Eng. 32, 100899 https://doi.org/10.1016/j.jwpe.2019.100899.
Karthikeyan, O.P., Visvanathan, C., 2013. Bio-energy recovery from high-solid organic substrates by dry anaerobic bio-conversion processes: A review. Rev. Environ. Sci. Biotechnol. 12, 257–284. https://doi.org/10.1007/s11157-012-9304-9.
Kayhanian, M., 1999. Ammonia Inhibition in High-Solids Biogasification: An Overview and Practical Solutions. Environ. Technol. 20, 355–365. https://doi.org/10.1080/09593332008616828.
Keppler, F., Laukenmann, S., Rinne, J., Heuwinkel, H., Greule, M., Whiticar, M., Lelieveld, J., 2010. Measurements of 13C/12C methane from anaerobic digesters: Comparison of optical spectrometry with continuous-flow isotope ratio mass spectrometry. Environ. Sci. Technol. 44, 5067–5073. https://doi.org/10.1021/es100460d.
Kim, D.H., Oh, S.E., 2011. Continuous high-solids anaerobic co-digestion of organic solid wastes under mesophilic conditions. Waste Manag. 31, 1943–1948. https://doi.org/10.1016/j.wasman.2011.05.007.
Kozich, J.J., Westcott, S.L., Baxter, N.T., Highlander, S.K., Schloss, P.D., 2013. Development of a Dual-Index Sequencing Strategy and Curation Pipeline for Analyzing Amplicon Sequence Data on the MiSeq Illumina Sequencing Platform. Appl. Environ. Microbiol. 79, 5112–5120. https://doi.org/10.1128/AEM.01043-13.
Kumar, M., Ou, Y.L., Lin, J.G., 2010. Co-composting of green waste and food waste at low C/N ratio. Waste Manag. 30, 602–609. https://doi.org/10.1016/j.wasman.2009.11.023.
Lai, M., 2019. Methanofollis, in: Bergey's Manual of Systematics of Archaea and Bacteria. Wiley, pp. 1–6. https://doi.org/10.1002/9781118960608.gbm00506.pub2.
Leng, L., Yang, P., Singh, S., Zhuang, H., Xu, L., Chen, W.H., Dolfing, J., Li, D., Zhang, Y., Zeng, H., Chu, W., Lee, P.H., 2018. A review on the bioenergetics of anaerobic microbial metabolism close to the thermodynamic limits and its implications for digestion applications. Bioresour. Technol. 247, 1095–1106. https://doi.org/10.1016/j.biortech.2017.09.103.
Li, J., Jha, A.K., Bajracharya, T.R., 2014. Dry Anaerobic Co-digestion of Cow Dung with Pig Manure for Methane Production. Appl. Biochem. Biotechnol. 173, 1537–1552. https://doi.org/10.1007/s12010-014-0941-z.

Liu, Y., Whitman, W.B., 2008. Metabolic, Phylogenetic, and Ecological Diversity of the Methanogenic Archaea. Ann. N. Y. Acad. Sci. 1125, 171–189. https://doi.org/10.1196/annals.1419.019.

Müller, N., Worm, P., Schink, B., Stams, A.J.M., Plugge, C.M., 2010. Syntrophic butyrate and propionate oxidation processes: from genomes to reaction mechanisms. Environ. Microbiol. Rep. 2, 489–499. https://doi.org/10.1111/j.1758-2229.2010.00147.x.

Ollivier, B.M., Mah, R.A., Garcia, J.L., Boone, D.R., 1986. Isolation and Characterization of Methanogenium bourgense sp. nov. Int. J. Syst. Bacteriol. 36, 297–301. https://doi.org/10.1099/00207713-36-2-297.

R Core Team, 2020. R: A Language and Environment for Statistical Computing.

Ripley, L.E., Boyle, W.C., Converse, J.C., 1997. Water environment federation. World Pumps 1997, 4. https://doi.org/10.1016/S0262-1762(99)80122-9.

Rocamora, I., Wagland, S.T., Villa, R., Simpson, E.W., Fernández, O., Bajón-Fernández, Y., 2020. Dry anaerobic digestion of organic waste: A review of operational parameters and their impact on process performance. Bioresour. Technol. 299, 122681 https://doi.org/10.1016/j.biortech.2019.122681.

Rocamora, I., Wagland, S.T., Rivas Casado, M., Hassard, F., Villa, R., Peces, M., Simpson, E.W., Fernández, O., Bajón-Fernández, Y., 2022a. Managing full-scale dry anaerobic digestion: Semi-continuous and batch operation. J. Environ. Chem. Eng. 10, 108154 https://doi.org/10.1016/j.jece.2022.108154.

Rocamora, I., Wagland, S.T., Villa, R., Simpson, E.W., Fernández, O., Bajón-Fernández, Y., 2022b. Use of Inoculum, Water and Percolate as Strategy to Avoid Inhibition on Dry-Batch Anaerobic Digestion of Organic Fraction of Municipal Solid Waste. Waste and Biomass Valorization 13, 227–239. https://doi.org/10.1007/s12649-021-01503-0.

Šafarič, L., Yekta, S.S., Svensson, B.H., Schnürer, A., Bastviken, D., Björn, A., 2020. Effect of cobalt, nickel, and selenium/tungsten deficiency on mesophilic anaerobic digestion of chemically defined soluble organic compounds. Microorganisms 8. https://doi.org/10.3390/microorganisms8040598.

Schink, B., 1997. Energetics of syntrophic cooperation in methanogenic degradation. Microbiol. Mol. Biol. Rev. 61, 262–280. https://doi.org/10.1128/mmbr.61.2.262-280.1997.

Schnürer, A., Nordberg, Å., 2008. Ammonia, a selective agent for methane production by syntrophic acetate oxidation at mesophilic temperature. Water Sci. Technol. 57, 735–740. https://doi.org/10.2166/wst.2008.097.

Schnürer, A., Zellner, G., Svensson, B.H., 1999. Mesophilic syntrophic acetate oxidation during methane formation in biogas reactors. FEMS Microbiol. Ecol. 29, 249–261. https://doi.org/10.1016/S0168-6496(99)00016-1.

Shams Esfandabadi, Z., Ranjbari, M., Scagnelli, S.D., 2022. The imbalance of food and biofuel markets amid Ukraine-Russia crisis: A systems thinking perspective. Biofuel Res. J. 9, 1640–1647. https://doi.org/10.18331/BRJ2022.9.2.5.

Siegert, I., Banks, C., 2005. The effect of volatile fatty acid additions on the anaerobic digestion of cellulose and glucose in batch reactors. Process Biochem. 40, 3412–3418. https://doi.org/10.1016/j.procbio.2005.01.025.

Song, H., Zhang, Y., Kusch-Brandt, S., Banks, C.J., 2020. Comparison of variable and constant loading for mesophilic food waste digestion in a long-term experiment. Energies 13, 1–14. https://doi.org/10.3390/en13051279.

Sprott, G.D., Patel, G.B., 1986. Ammonia toxicity in pure cultures of methanogenic bacteria. Syst. Appl. Microbiol. 7, 358–363. https://doi.org/10.1016/S0723-2020(86)80034-0.

Sprott, G.D., Shaw, K.M., Jarrell, K.F., 1984. Ammonia/potassium exchange in methanogenic bacteria. J. Biol. Chem. 259, 12602–12608. https://doi.org/10.1016/S0021-9258(18)90789-1.

Stams, A.J.M., Plugge, C.M., 2009. Electron transfer in syntrophic communities of anaerobic bacteria and archaea. Nat. Rev. Microbiol. 7, 568–577. https://doi.org/10.1038/nrmicro2166.

Suksong, W., Kongjan, P., Prasertsan, P., O-Thong, S.,, 2019. Thermotolerant cellulolytic Clostridiaceae and Lachnospiraceae rich consortium enhanced biogas production from oil palm empty fruit bunches by solid-state anaerobic digestion. Bioresour. Technol. 291, 121851 https://doi.org/10.1016/j.biortech.2019.121851.

Sun, L., Pope, P.B., Eijsink, V.G.H., Schnürer, A., 2015. Characterization of microbial community structure during continuous anaerobic digestion of straw and cow manure. Microb. Biotechnol. 8, 815–827. https://doi.org/10.1111/1751-7915.12298.

Tian, G., Xi, J., Yeung, M., Ren, G., 2020. Characteristics and mechanisms of H2S production in anaerobic digestion of food waste. Sci. Total Environ. 724, 137977 https://doi.org/10.1016/j.scitotenv.2020.137977.

Tidjani Alou, M., Khelaifia, S., Michelle, C., Andrieu, C., Armstrong, N., Bittar, F., Sokhna, C., Diallo, A., Fournier, P.-E., Raoult, D., Million, M., 2016. Anaerococcus rubiinfantis sp. nov., isolated from the gut microbiota of a Senegalese infant with severe acute malnutrition. Anaerobe 40, 85–94. https://doi.org/10.1016/j.anaerobe.2016.06.007.

Tsui, T., Zhang, L., Zhang, J., Dai, Y., Tong, Y.W., 2022. Engineering interface between bioenergy recovery and biogas desulfurization: Sustainability interplays of biochar application. Renew. Sustain. Energy Rev. 157, 112053 https://doi.org/10.1016/j.rser.2021.112053.

Vrieze, J. De, Hennebel, T., Boon, N., Verstraete, W., 2012. Methanosarcina: The rediscovered methanogen for heavy duty biomethanation. Bioresour. Technol. 112, 1–9. https://doi.org/https://doi.org/10.1016/j.biortech.2012.02.079.

Westerholm, M., Levén, L., Schnürer, A., 2012. Bioaugmentation of Syntrophic Acetate-Oxidizing Culture in Biogas Reactors Exposed to Increasing Levels of Ammonia. Appl. Environ. Microbiol. 78, 7619–7625. https://doi.org/10.1128/AEM.01637-12.

Westerholm, M., Müller, B., Isaksson, S., Schnürer, A., 2015. Trace element and temperature effects on microbial communities and links to biogas digester performance at high ammonia levels. Biotechnol. Biofuels 8, 154. https://doi.org/10.1186/s13068-015-0328-6.

Westerholm, M., Dolfing, J., Schnürer, A., 2019. Growth Characteristics and Thermodynamics of Syntrophic Acetate Oxidizers. Environ. Sci. Technol. 53, 5512–5520. https://doi.org/10.1021/acs.est.9b00288.

Whiticar, M.J., 1999. Carbon and hydrogen isotope systematics of bacterial formation and oxidation of methane. Chem. Geol. 161, 291–314. https://doi.org/10.1016/S0009-2541(99)00092-3.

Whiticar, M., Faber, E., Schoell, M., 1986. Biogenic methane formation in marine and freshwater environments: CO2 reduction vs. acetate fermentation—Isotope evidence. Geochim. Cosmochim. Acta 50, 693–709. https://doi.org/10.1016/0016-7037(86)90346-7.

Xu, S., Han, R., Zhang, Y., He, C., Liu, H., 2018. Differentiated stimulating effects of activated carbon on methanogenic degradation of acetate, propionate and butyrate. Waste Manag. 76, 394–403. https://doi.org/10.1016/j.wasman.2018.03.037.

Yan, M., Treu, L., Zhu, X., Tian, H., Basile, A., Fotidis, I.A., Campanaro, S., Angelidaki, I., 2020. Insights into Ammonia Adaptation and Methanogenic Precursor Oxidation by Genome-Centric Analysis. Environ. Sci. Technol. 54, 12568–12582. https://doi.org/10.1021/acs.est.0c01945.

Yan, Y., Yan, M., Ravenni, G., Angelidaki, I., Fu, D., Fotidis, I.A., 2022. Novel bioaugmentation strategy boosted with biochar to alleviate ammonia toxicity in continuous biomethanation. Bioresour. Technol. 343, 126146 https://doi.org/10.1016/j.biortech.2021.126146.

Yirong, C., Zhang, W., Heaven, S., Banks, C.J., 2017. Influence of ammonia in the anaerobic digestion of food waste. J. Environ. Chem. Eng. 5, 5131–5142. https://doi.org/10.1016/j.jece.2017.09.043.

Zeshan, K., O.P., Visvanathan, C.,, 2012. Effect of C/N ratio and ammonia-N accumulation in a pilot-scale thermophilic dry anaerobic digester. Bioresour. Technol. 113, 294–302. https://doi.org/10.1016/j.biortech.2012.02.028.

Zhang, Y., Banks, C.J., Heaven, S., 2012. Co-digestion of source segregated domestic food waste to improve process stability. Bioresour. Technol. 114, 168–178. https://doi.org/10.1016/j.biortech.2012.03.040.